

University of Texas Rio Grande Valley

ScholarWorks @ UTRGV

Physics and Astronomy Faculty Publications
and Presentations

College of Sciences

2006

Electrical pulse formation during high temperature reaction between Ni and Al

Mona Setoodeh

Karen S. Martirosyan

The University of Texas Rio Grande Valley

Dan Luss

Follow this and additional works at: https://scholarworks.utrgv.edu/pa_fac



Part of the [Astrophysics and Astronomy Commons](#), and the [Physics Commons](#)

Recommended Citation

Setoodeh, Mona; Martirosyan, Karen S.; and Luss, Dan, "Electrical pulse formation during high temperature reaction between Ni and Al" (2006). *Physics and Astronomy Faculty Publications and Presentations*. 343. https://scholarworks.utrgv.edu/pa_fac/343

This Article is brought to you for free and open access by the College of Sciences at ScholarWorks @ UTRGV. It has been accepted for inclusion in Physics and Astronomy Faculty Publications and Presentations by an authorized administrator of ScholarWorks @ UTRGV. For more information, please contact justin.white@utrgv.edu, william.flores01@utrgv.edu.

Electrical pulse formation during high temperature reaction between Ni and Al

Mona Setoodeh, K. S. Martirosyan, and Dan Luss^{a)}

Department of Chemical Engineering, University of Houston, Houston, Texas 77204-4792

(Received 16 August 2005; accepted 24 February 2006; published online 18 April 2006)

An electric voltage pulse (duration of about 2 ms) with an amplitude of up to 0.6 V was generated during the reaction between nickel and aluminum powders by a high temperature moving reaction front. The electrical signal formed during the initial stages of the combustion was annihilated before the moving front attained its maximum temperature. The voltage amplitude and combustion temperature depended on the particle size of the reactants as well as the Al to Ni ratio in the reactant mixture, and their largest values were attained for a mixture containing 27–31.5 wt % Al. The combustion temperature increased when smaller Al particles were used. The electric signals annihilated either due to the growth of the initially formed product layer and/or as a result of the formation of a molten Al matrix as the reaction propagated. Oscillatory signals formed during unstable combustion in which the reaction front was perturbed. Unipolar and nonoscillating signals formed when the combustion front was planar. We conjecture that the electric field was generated by the different diffusion rates of charge carriers through a reaction generated thin exterior intermediate products shell of $\text{Al}_3\text{Ni}/\text{Al}_3\text{Ni}_2$. © 2006 American Institute of Physics.

[DOI: 10.1063/1.2188028]

INTRODUCTION

Experimental and theoretical investigations revealed that an electromagnetic field is generated during gas-solid combustion of metals.^{1–10} Electrical and magnetic fields have been detected during both oxidation^{1–5} and nitridation of pure metal particles.^{6–8} Electrical fields of about 2 V and 100 mA formed during the initial stages of oxidation of single metal particles of Zr, Ti, Fe, and Ni ($\varnothing=0.8$ mm).⁹ The different diffusion fluxes of positive and negative charge carriers through a growing mixed ionic-electronic conducting shell of intermediate products were the main reason for the generation of the electrical field.^{9,11}

Many self-propagating high-temperature synthesis (SHS) reactions involve solid-solid reactions. The mechanism of self-sustaining high temperature solid-solid reactions is much more intricate than that of gas-solid reactions. High temperature solid-solid reactions on the other hand consist of melting of one or more of the reactants and/or products, dissolution of reactants and/or intermediate phases, crystallization and precipitation of the products from the liquid phase, and evolution of the microstructure. Prediction of the solid-solid reaction behavior is complicated as the reaction rate, microstructure of the products, and combustion front velocity are highly affected by the reactant particle size.^{12,13} Kinetic models that predict the dependence of the reaction rate on the temperature, feed composition, and particle size of the reactants are not yet available for most solid-solid reactions.

The goal of this study was to determine if an electrical field can form during some solid-solid reactions, and what its characteristic features, such as magnitude and duration, are. We selected as a test reaction the combustion synthesis of

NiAl from a mixture of Ni and Al powders due to its relatively low combustion temperature which helps avoid melting of the Pt electrodes and thermocouples.¹⁴ Although the combustion synthesis of NiAl is referred to as a solid-solid combustion, it is a heterogeneous reaction. It involves melting of one reactant (Al) and proceeds both in the molten phase and in the solid particles. After an initial period, the reaction proceeds essentially in the liquid phase. While this reaction has been extensively studied, no established mechanism exists that accounts for the detailed kinetics involved in the various reaction steps, the rate of dissolution of the two reactants in each other (before a continuous molten Al phase forms), and the impact of the reactant particle size. This missing information is needed to enable prediction of the electric field formation and its characteristic features.

We studied the simultaneous evolution of the temperature and the electrical voltage during the combustion synthesis of NiAl over a range of reactant mixture compositions and particle size. We propose a possible mechanism for the electric field formation. The dependence of the electric fields on factors such as reactant mixture composition and reactant particle size is discussed.

EXPERIMENTAL SETUP AND PROCEDURE

The reaction was conducted in a ceramic boat located inside a bell-shaped, quartz reactor purged with argon (99.99%). The experimental setup, the top view of which is shown schematically in Fig. 1, consists of a voltmeter, an ammeter, and a thermocouple signal recorder. The temperature and electrical signals were measured by a data acquisition system (Omega, Inc.) and recorded on a PC. The electric voltage was measured by a pair of Pt or W electrodes ($\varnothing=0.125$ mm) located at a distance of about 2 mm from each other and normal to the direction of the moving combustion

^{a)}Electronic mail: dluss@uh.edu

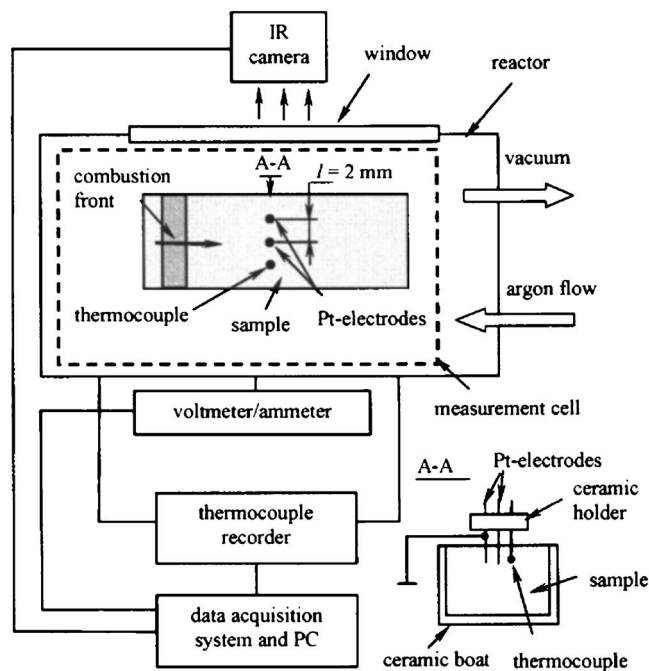


FIG. 1. Schematic of the experimental setup.

front. An *S*-type (Pt/Pt–Rh) ($\varnothing=0.1$ mm) thermocouple was used to measure the temperature during the reaction. The electrodes and/or thermocouple were located at a depth of 2 mm below the surface of the sample. In one experiment the electrodes and the thermocouple were located 1 mm above the sample's surface in order to detect any possible electrical field in the gas phase. The impedance during the voltage and current measurements were 0.25 M Ω and 0.1 Ω , respectively. This arrangement of the thermocouple and the electrodes, proposed in Ref. 15, enabled simultaneous measurements of temperature and electric voltage/current in a plane perpendicular to the moving combustion front. This setup overcomes experimental problems associated with using electrodes that are located at a certain distance along the direction of the propagating combustion front, such as having the electrodes exposed to different temperatures and different compositions. The shape and velocity of the combustion front were followed by an IR digital video camera [Merlin Mid InSb infrared (MWIR) camera, Indigo Systems]. The sample was placed in a ceramic boat similar to that used during the electric field measurements. The boat was placed inside a stainless steel cylindrical vessel with a sapphire window. The vessel was purged by argon during the combustion.

The green charge was a powder mixture of 20–50 wt % Al (97.5% pure, Alfa Aesar Inc.) and 50–80 wt % Ni (99.9% pure, Alfa Aesar Inc.). Two different Al powders (average particle sizes of about 10 and 70 μm) and two Ni powders (about 10 and 70 μm) were used. The reactant powders were mixed for 30 min in mixer/mill machine (CertiPrep, Inc.), using 1/4 in. 316 stainless balls. Approximately 10 g of the loose sample was loaded into a $10 \times 10 \times 80$ mm³ ceramic boat. The reactant mixture was ignited by an electrically heated coil, the width of which was equal to that of the ceramic boat in order to initiate a planar combustion front.

The electric current to the ignition coil was terminated immediately after ignition to prevent electrical interference during the measurements.

Quenching experiments were conducted in a cylindrical copper block 72 mm in diameter and 62 mm in length. The sample was placed in a cone inside the block. The diameter of the base of the cone was 20 mm. The mass of the copper block (2.5 kg) was much larger than that of the samples (about 40 g), providing rapid heat removal from the sample (thermal conductivity of Cu is about 400 W/m K). The block was located under a bell-shaped vessel which was first vacuumed and then filled with argon. The sample was ignited with an electrically heated coil at the base of the sample cone. The combustion was extinguished at a critical position, at which the heat losses prevented the front from propagating any further.¹⁶

The phase composition of the products was determined by x-ray diffraction (XRD) (Siemens D5000; Cu $K\alpha$ radiation source). The microstructure of the product was analyzed using scanning electron microscopy (SEM) (Jeol, Inc.).

EXPERIMENTAL RESULTS

The temporal electric voltage, current, and temperature in a moving temperature front were simultaneously measured during the solid-solid combustion synthesis,



where x is the stoichiometric coefficient of Al. The moving combustion front was not planar and its velocity was not constant when the reactant mixture consisted of Ni and Al powders with an average particle size of about 70 μm . The corresponding electric voltage oscillated and was not reproducible. The combustion temperature exceeded 2000 $^\circ\text{C}$ when the green mixture consisted of Ni and Al powders with an average particle size of about 10 μm . This high temperature caused partial melting of the thermocouples so that precise temperature measurements were not feasible. The corresponding velocity of the moving combustion front was relatively high (3–4 cm/s), and the electrical signal duration was very short, of the order of 1 ms. This short duration was the lowest detection limit of our measurement equipment. Thus, reproducible data could not be obtained using these powders.

Successful measurements of the electric voltage and temperature were possible when the average particle size of one reactant powder was significantly larger than that of the second, i.e., using mixtures of 70 μm Al and 10 μm Ni particles, or of 10 μm Al and 70 μm Ni particles. Figure 2 shows the temporal electric voltage and temperature generated by a planar combustion front of a mixture containing 25 wt % Al/75 wt % Ni for the two mixtures with the different particle size distributions. In both cases the electric signal was generated and annihilated before the maximum combustion temperature was achieved. The duration of the electric signal (order of ms) was much shorter than that of the temperature rise (order of seconds). The maximum voltage for a mixture of 70 μm Al and 10 μm Ni particles was about 0.5 V [Fig. 2(a)] and it lasted for about 10 ms. It was

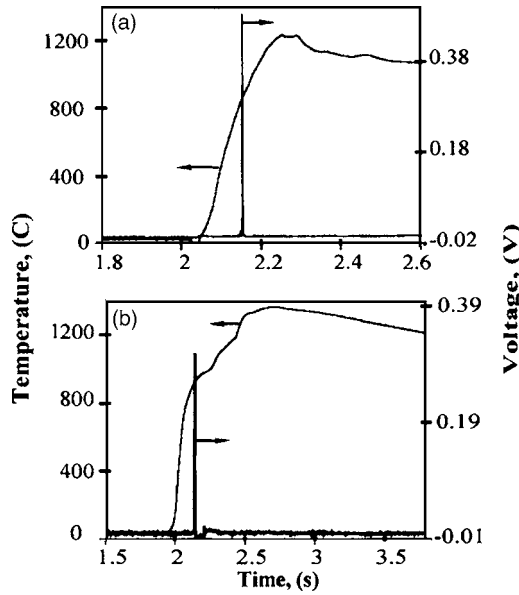


FIG. 2. Simultaneous measurements of the combustion temperature and the electric voltage. Reactant mixture: Al/Ni 25/75 wt %. Distance between Pt electrodes is 2 mm. Average particle sizes of reactant powders: (a) Al, 70 μm ; Ni, 10 μm ; and (b) Al, 10 μm , Ni, 70 μm .

generated at a temperature of about 900 $^{\circ}\text{C}$, 0.1 s after the beginning of the temperature rise and 0.1 s before the maximum combustion temperature of 1220 $^{\circ}\text{C}$ was attained. The combustion front moved at a velocity of about 1.5 cm/s. The maximum voltage for a mixture of 10 μm Al and 70 μm Ni particles was about 0.3 V [Fig. 2(b)] and its duration was 25 ms. It was generated at a temperature of about 960 $^{\circ}\text{C}$, 0.16 s after the beginning of the temperature rise and 0.5 s before the maximum combustion temperature of 1360 $^{\circ}\text{C}$ was attained. The combustion front moved at a velocity of about 2 cm/s. The measured electrical current for both reactant mixtures was about 50 mA. A negligible electrical voltage (Fig. 3) was detected in the gas phase close to the sample surface during the combustion of a mixture consisting of 31.5 wt % Al (10 μm) and 68.5 wt % Ni (70 μm).

The particle size affected the range of the green charge

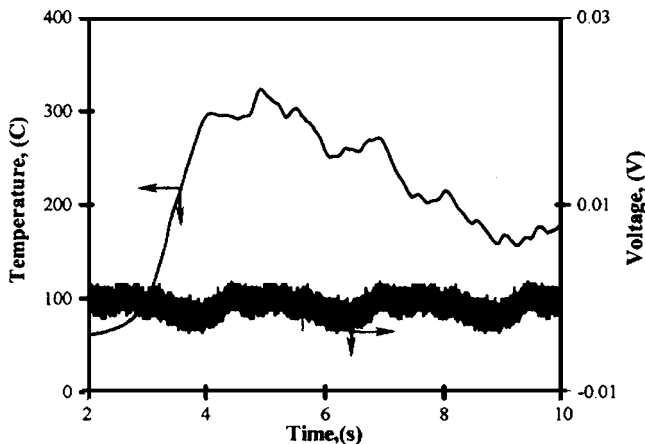


FIG. 3. Simultaneous measurements of the temperature and electric voltage in the gas phase. Reactant mixture: Al (70 μm) of 31.5 wt % and Ni (10 μm) of 68.5 wt %. Distance between the electrodes is 2 mm. The electrodes are located 2 mm above the sample surface.

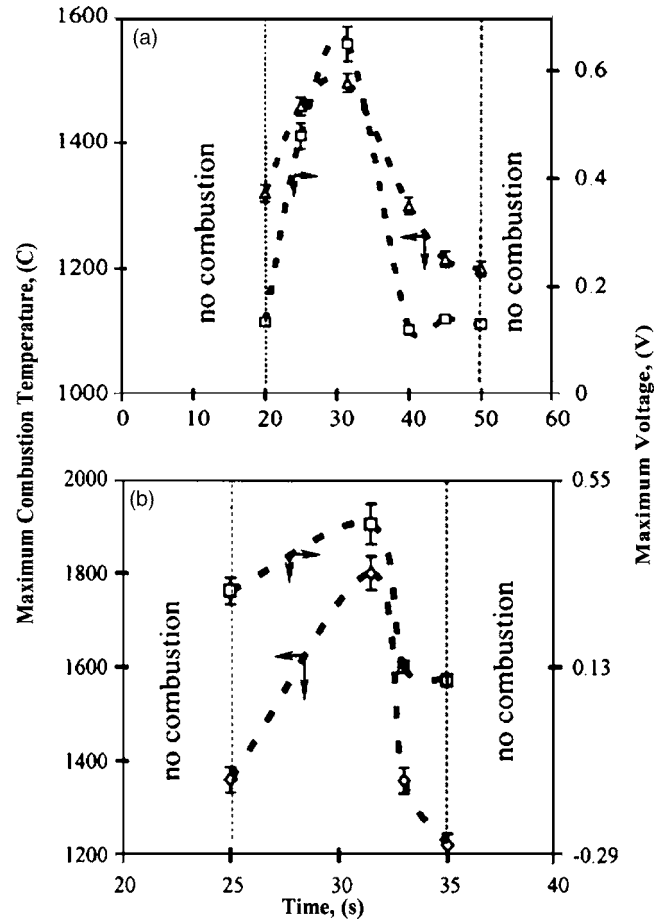


FIG. 4. Effect of Al wt % in the reactant mixture on the maximum combustion temperature and electrical voltage. (a) Al and Ni particle sizes: 70 and 10 μm , respectively; (b) Al and Ni particle sizes: 10 and 70 μm , respectively.

composition over which a stable combustion could be obtained. The combustion could be initiated and sustained for a reactant mixture consisting of 20–50 wt % Al with the Al and Ni powders having average sizes of 70 and 10 μm , respectively. The combustion could be initiated and sustained for a reactant mixture containing 25–35 wt % Al when the average particle sizes of the Al and Ni powders were 10 and 70 μm , respectively. The moving combustion front was planar and propagated at a constant velocity of 1–3 cm/s depending on the green charge composition. The electric signals were unipolar. The moving combustion front and the electric signals oscillated when the mixture composition was close to that at which extinction occurred. It was rather difficult to sustain the combustion close to these limiting compositions.

The maximum electrical field and combustion temperature depended on the initial composition. For both mixtures the maximum electric voltage and combustion temperature were obtained for reactant mixtures containing 27–31.5 wt % Al (Fig. 4). For the same reactant mixture composition the combustion temperature obtained when fine Al (10 μm) and coarse Ni (70 μm) powders were utilized was higher than that for the mixture with coarse Al (70 μm) and fine Ni (10 μm). The qualitative dependence of the maximum electric voltage on the composition of the reactant mixture was similar for both mixtures.

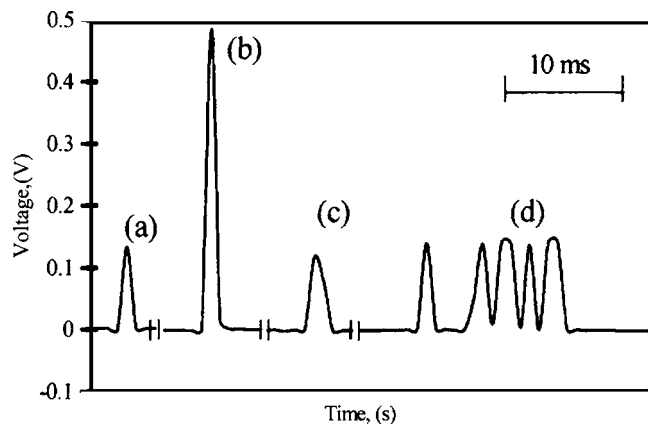


FIG. 5. Effect of Al wt % in the reactant mixture on the generated electric voltage. Al and Ni particle sizes: 70 and 10 μm , respectively. (a) Al/Ni (20/80); (b) Al/Ni (25/75); (c) Al/Ni (40/60); (d) Al/Ni (50/50).

The temporal electrical voltage depended on the composition of the reactant mixture (Fig. 5) while the duration of the signals (about 2 ms) did not. A sequence of several electrical pulses formed close to the extinction temperature [case (d) in Fig. 5]. The shape and velocity of the moving combustion front were determined by the IR camera for a mixture of 50 wt % Al (70 μm) and 50 wt % Ni (10 μm). Figure 6 shows that the oscillation of the electrical field [Fig. 5(d)] was related to the oscillations in the combustion front movement. The average velocity of the combustion front was 1.5 cm/s.

A quenching front experiment was conducted to determine the temporal phase and composition changes by the propagating reaction front for a mixture containing 31.5 wt % Al and 68.5 wt % Ni. The average particle sizes of

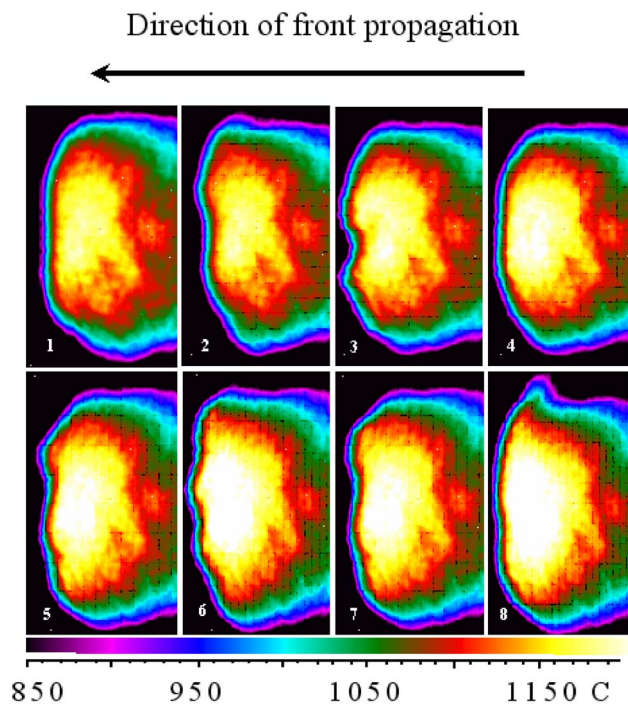


FIG. 6. (Color online) Temporal IR images of the sample surface during combustion for a mixture of 50 wt % Al (70 μm) and 50 wt % Ni (10 μm).

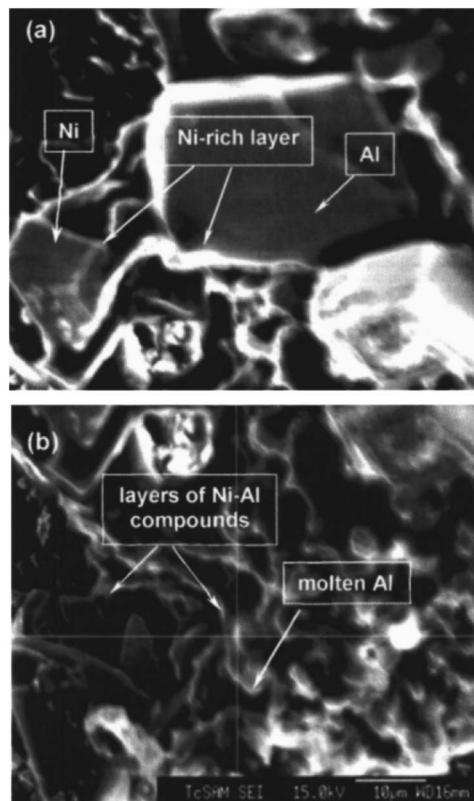


FIG. 7. The SEM images of the quenched front. Reactant mixture: Al/Ni 31.5/68.5 wt %. Al and Ni particle sizes: 70 and 10 μm , respectively. (a) At the tip of quenched cone; (b) at a distance of 8 mm from the tip.

the Al and Ni powders were 70 and 10 μm , respectively. The microstructure and composition of the quenched cone products were determined by SEM analysis and XRD at several horizontal cross sections. Figure 7(a) is a SEM image obtained at the tip of the quenched cone. It shows an unreacted Ni core surrounded by a layer of Ni-rich compounds as well as unreacted Ni and Al particles. Molten Al/Al-rich phase and thin layers of Ni-Al compounds were located at a distance of 8 mm from the tip of the quenched front [Fig. 7(b)]. As the front velocity was about 3 cm/s, this transformation took about 0.26 s. The XRD patterns obtained at several locations of the cone (Fig. 8) showed that with increasing distance from the quenched tip (the tip is the location at which the combustion front extinguishes and the green mixture consists of unreacted Ni and Al powders), the intensity of the Ni and Al peaks decreased and eventually vanished while Ni_2Al_3 and NiAl peaks appeared and their intensities increased. Even though the reactant mixture was an equimolar composition of NiAl the final product consisted of both NiAl and Al_3Ni_2 as well as small amounts of unreacted Ni and Al.

DISCUSSION

A thermoemission from a homogeneous surface generates a current density (J_e) that satisfies the Richardson-Dushman relation¹⁷

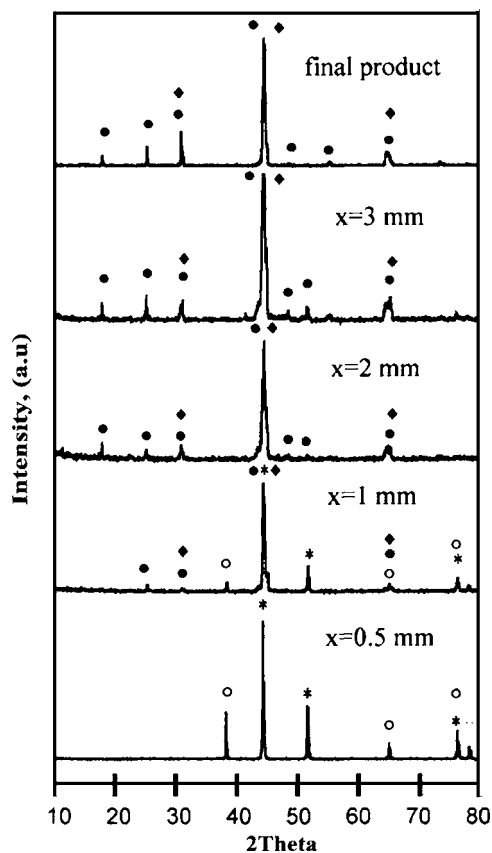


FIG. 8. XRD pattern of the quenched front. Reactant mixture: 31.5 wt % Al (70 μm)/68.5 wt % Ni (10 μm). Key: (*) Ni, (O) Al, (●) Al_3Ni_2 , (□) Al_3Ni , and (◆) NiAl.

$$J_e = (1 - \bar{k})A_0T^2 \exp(-\phi/KT), \quad (2)$$

where \bar{k} is the electron reflection coefficient, $A_0 = 4\pi me k^2/h^3 = 1.204 \times 10^6 \text{ A m}^{-2} \text{ K}^{-2}$, and ϕ is the solid work function. The work functions of Ni, Al, and Pt are 5.15, 4.2, and 5.65 eV, respectively. The predicted value of J_e at a temperature of 1500 °C and at $\bar{k}=0$ is about $2 \times 10^{-3} \text{ A/cm}^2$ for these materials. This value is much smaller than the measured current density of about 1.6 A/cm². The current density is calculated by dividing the measured electrical current (50 mA) by the surface area of the electrodes (0.03 cm²). An electrical potential formed by thermoelectric phenomenon also increases monotonically with temperature. It is estimated to be of the order of 20–35 mV at 1500 °C for S-type thermocouples¹⁸ which is smaller than the measured electric voltage during the combustion by about two orders of magnitude. In all the experiments a short electrical voltage pulse formed during the initial stages of the reaction (Fig. 2). The annihilation of the temporal voltage signal well before the temperature reached its maximum suggests strongly that neither the high temperature electron thermal emission nor the thermoelectric phenomenon were the dominant mechanism generating the electrical signals. Also no electric signal was generated by the thermoelectric phenomenon as can be seen in Fig. 3.

The detailed mechanism of the reaction between Ni and Al during combustion synthesis is rather complex as it involves melting of at least one of the reactants (Al) and pro-

ceeds both in the molten phase and the solid particles. After an initial period, a transition occurs from a solid-phase reaction to one in the liquid phase. Many investigations of the mechanism of the combustion synthesis of NiAl have been reported,^{12,18–23} using various experimental techniques such as time-resolved x-ray diffraction (TRXRD),²¹ layer wise analysis of the microstructure of a quenched front,²³ and real-time electron microscopy.²⁰ Yet, there is no established model that predicts the dependence of the reaction rate on the temperature, feed composition, and particle size. The studies by Aleksandrov and Korchagin²⁴ and Biswas and Roy²³ indicate that the reaction mechanism is a dissolution-precipitation and only a partial conversion is achieved in the combustion zone. The conversion of the solid reactants to products is completed several seconds after the passage of the high temperature moving front.

Previous studies suggest that during the SHS of a mixture of coarse Ni and fine Al particles, heat conduction caused partial melting of the Al. Dissolution of Al in the exterior layer of the solid Ni particles caused formation of an Al_3Ni product shell at the surface of Ni particles.²³ The reaction mechanism is similar when Al particles larger than Ni particles are utilized, except that the formation of the initial product layer is due to the dissolution of Ni in the molten Al.¹² This product layer is clearly observed in the SEM images obtained at the quenched front [Fig. 7(a)]. A NiAl matrix is formed next and the unreacted Ni is transformed to a Ni (Al)– Al_3Ni eutectic.²³ During the early stage of the reaction the melting of the Al particles is not complete and the Ni particles are not submerged in a continuous matrix of molten Al. Eventually all the Al particles melt, forming a continuous phase in which the Ni particles are submerged. The reaction then proceeds mainly by dissolution and reaction of the Ni in the molten Al-rich phase.^{12,23} Following the formation of NiAl in the molten Al phase, it crystallizes and precipitates from the saturated liquid.²³

The electrical signal formed during the initial stage of the combustion before a continuous matrix of molten Al existed between the two electrodes. During this initial period only a fraction of the Al particles was molten and the Ni particles were surrounded by a thin shell of Al_3Ni and/or Al_3Ni_2 . The electrical signal formed rather shortly (0.1–0.15 s, Fig. 2) after the temperature started to rise. This short time span was probably not sufficient for the complete melting of all Al particles. A comparison between the XRD patterns and the SEM images of the quenched front, and the delay time between the temperature rise and electric field formation indicated that the electric fields were formed in a region where the sample consisted of an unreacted Ni core and a shell of intermediates, namely, Al_3Ni and Al_3Ni_2 . We conjecture that the different diffusion rates of charge carriers through this product shell generated a double charged layer which caused the formation of the electrical pulse. Previous studies of the reaction mechanism between Ni and Al (Refs. 12, 20, and 23–26) suggested that Al and Ni diffuse through the initial product shell as neutral atoms. Also, the ionization energy of both Ni (718 kJ/mol) and Al (567 kJ/mol) are higher than the heat of the reaction (50–60 kJ/mol) between them. Therefore, we conjecture that the charge carriers

formed during the combustion synthesis of NiAl are electrons and electron holes, generated via thermal ionization $e^- + h^+ \leftrightarrow \text{nil}$ at the surface. The free electron density of Al ($1.81 \times 10^{23}/\text{cm}^3$) is larger than that of Ni ($1.1 \times 10^{22}/\text{cm}^3$) by an order of magnitude.²⁷ This difference in electron concentration is the driving force of the electron migration across the product layer which can generate a double charged layer across the product shell.

The thickness of the double layer is approximately

$$h_d = \sqrt{\int_{T_0}^T D_i(T) \left(\frac{dt}{dT} \right) dt}, \quad (3)$$

where $D_i = 3.59 \exp(-303 \text{ kJ/mol}/RT) \text{ cm}^2/\text{s}$ is the temperature dependent diffusion coefficient of the Ni in Ni_3Al .²⁵ In our experiments $dt/dT \approx 1/2500 \text{ s/K}$. In the temperature range of 800–1200 °C, the diffusion layer is of the order of 10^{-6} m . The characteristic scale of the electric field is the Debye screening length (D_l), the magnitude of which is calculated by the relation

$$D_l = \sqrt{\frac{kT}{4\pi e^2 N}}, \quad (4)$$

where k is the Boltzmann constant, T the temperature, e the electron charge, and N the free electron density (of the order of 10^{22} – 10^{23} cm^{-3}). The corresponding Debye screening length is about 10^{-6} – 10^{-5} m . The maximum electrical potential is obtained when the thickness of the Debye screening length exceeds that of the initial product shell (h_i) of Al_3Ni and Al_3Ni_2 . In that case a charge separation occurs across the entire product layer. In our experiments as the thickness of the product layer increases and exceeds that of the Debye screening length ($h_d > D_l$) the charge separation occurs only across part of the product layer, resulting in a decrease and eventually annihilation of the electrical signal. Another reason for the voltage extinction is that after a certain time a continuous molten Al phase forms. The electrical voltage vanishes once all the solid Ni particles are submerged in the molten Al-rich phases.

The combustion temperature depends on the Al to Ni ratio in the reactant mixture. Its maximum value was attained when the concentration of the reactant mixtures was close to the stoichiometric concentration of NiAl, i.e., 31.5 wt % Al (Fig. 3). This finding agrees with the report by Nash and Kleppa²⁸ that the maximum formation enthalpy of $\text{Ni}_{(1-y)}\text{Al}_y$ ($\sim 60 \text{ kJ/mol}$) occurs at $0.48 < y < 0.5$. This product is obtained from a reactant mixture with 25–32 wt % of Al.

The dependence of the maximum electric voltage and the maximum reaction temperature on the reactant composition was similar for both reactant powder mixtures (Fig. 4). A possible explanation is that increasing the temperatures leads to a higher rate of generation of charge carriers at the particle surface, which in turn increases the maximum value of the electric voltage pulse.

For the same initial composition, the combustion temperature was higher when mixtures with small Al particles were utilized. The smaller Al particles melt faster than the large ones and this led to a higher reaction rate and a larger rate of heat release.¹³ Also smaller size particles store much

higher enthalpy per unit volume which accelerates the reaction process as it facilitates the diffusion and the melting of Al.

When reactant mixtures with Al to Ni ratios close to that causing the extinction of the combustion front were used, the unstable combustion front generated oscillatory electric signals. The IR images of the combustion front revealed that the oscillations in the electrical signals [Fig. 5, case (d)] are probably caused by perturbations in the moving combustion front (Fig. 6).

The XRD revealed that although the stoichiometric composition of the green charge corresponded to NiAl, the conversion was not complete and the product consisted of both NiAl and Al_3Ni_2 . This may be due to usage of coarse particles in the green charge, which decreased the contact between the particles and increased the migration distance between the Ni and Al atoms. This decreased the reaction rate. Consequently, small amounts of Al and Ni-rich liquid and droplets remain in the sample and crystallize as Al– Al_3Ni eutectic and Al_3Ni_2 phases.

CONCLUSIONS

Transient electrical voltages of up to 0.6 V with durations of about 2 ms were generated during the initial period of combustion synthesis of NiAl. The maximum voltage and temperature depended on the particle size of the reactants as well as the composition of the reactant mixture, and their largest values were attained during the combustion of a mixture containing 27–31.5 wt % Al. For the same reactant composition the combustion temperature was higher when smaller Al particles were used. Perturbations in the front generated oscillatory electric signals. We conjecture that the voltage pulse was formed due to the different diffusive velocities of charge carriers across the product shell. We suggest the charge carriers generated in the system to be electrons and electron holes which migrate through the initially formed product layer of $\text{Al}_3\text{Ni}/\text{Al}_3\text{Ni}_2$ with different diffusive velocities, forming a double charged layer across each particle. The annihilation of the signals is caused either by the growth of the initially formed product layer and its thickness exceeding that of the Debye screening length, or by formation of a continuous matrix of molten Al as the reaction proceeds.

ACKNOWLEDGMENTS

We acknowledge the financial support of the research by the National Science Foundation and the assistance of the Materials Research Science and Engineering Centre at the University of Houston.

¹M. D. Nersesyan, J. R. Claycomb, Q. Ming, J. H. Miller, J. T. Richardson, and D. Luss, *Appl. Phys. Lett.* **75**, 1170 (1999).

²K. S. Martirosyan, J. R. Claycomb, G. Gogoshin, R. A. Yabrough, J. H. Miller Jr., and D. Luss, *J. Appl. Phys.* **93**, 9329 (2003).

³J. R. Claycomb, W. LeGrand, J. H. Miller Jr., M. D. Nersesyan, J. T. Ritchie, and D. Luss, *Physica C* **341**, 2641 (2000).

⁴K. S. Martirosyan, J. R. Claycomb, J. H. Miller Jr., and D. Luss, *J. Appl. Phys.* **96**, 4632 (2004).

⁵I. Filimonov and D. Luss, *AIChE J.* **51**, 1521 (2005).

⁶Y. G. Morozov, M. V. Kuznetsov, M. D. Nersesyan, and A. G. Merzhanov,

- Dokl. Akad. Nauk **351**, 780 (1996).
- ⁷V. A. Kurdyashov, A. S. Mukasyan, and I. A. Filimonov, *J. Mater. Synth. Process.* **4**, 353 (1996).
- ⁸K. S. Martirosyan, M. Setoodeh, and D. Luss, *J. Appl. Phys.* **98**, 054901 (2005).
- ⁹K. S. Martirosyan, I. A. Filimonov, M. D. Nersesyan, and D. Luss, *J. Electrochem. Soc.* **150**, J9 (2003).
- ¹⁰H. Rode, D. Orlicki, and V. Hlavacek, *AIChE J.* **41**, 2614 (1995).
- ¹¹K. S. Martirosyan, I. A. Filimonov, and D. Luss, *AIChE J.* **50**, 241 (2004).
- ¹²Q. Fan, H. Chai, and Z. Jin, *Intermetallics* **9**, 609 (2001).
- ¹³S. Dong, P. Hou, H. Yang, and G. Zou, *Intermetallics* **10**, 217 (2002).
- ¹⁴L. Farber, I. Gotman, and E. Y. Gutmanas, *Mater. Res. Soc. Symp. Proc.* **460**, 561 (1997).
- ¹⁵K. S. Martirosyan, I. A. Filimonov, and D. Luss, *Int. J. Self-Propag. High-Temp. Synth.* **11**, 325 (2002).
- ¹⁶A. Rogachev, A. S. Mukasyan, and A. Varma, *Combust. Sci. Technol.* **175**, 357 (2003).
- ¹⁷T. S. Hutchison and D. S. Barid, *The Physics of Engineering Solids* (Wiley, New York, 1963).
- ¹⁸H. G. Goldschmidt, *Interstitial Alloys* (Butterworths, London, 1967), p. 296.
- ¹⁹S. Dong, P. Hou, H. Cheng, H. Yang, and G. Zou, *J. Phys.: Condens. Matter* **14**, 11023 (2002).
- ²⁰Y. Zhang and G. C. Stangle, *J. Mater. Res.* **10**, 962 (1995).
- ²¹A. S. Rogachev, B. P. Tolochko, N. Z. Lyakhov, M. P. Sharafutdinov, N. A. Popkov, B. Ya. Pirogov, and E. B. Pis'menskaya, *Crystallogr. Rep.* **48**, 466 (2003).
- ²²F. Bernard, E. Gaffet, M. Gramond, M. Gailhanou, and J. C. Gachon, *J. Synchrotron Radiat.* **7**, 27 (2000).
- ²³A. Biswas and S. K. Roy, *Acta Mater.* **52**, 257 (2004).
- ²⁴V. V. Aleksandrov and M. A. Korchagin, *Combust., Explos. Shock Waves* **24**, 557 (1988).
- ²⁵C. Cserhati, A. Paul, A. A. Kodenstov, M. J. H. van Dal, and F. J. J. van Loo, *Intermetallics* **11**, 291 (2003).
- ²⁶J. C. Liu and J. W. Mayer, *J. Appl. Phys.* **64**, 656 (1968).
- ²⁷N. W. Ashcroft and N. D. Mermin, *Solid State Physics* (Brooks-Cole, Belmont, MA, 1976).
- ²⁸P. Nash and O. Kleppa, *J. Alloys Compd.* **321**, 228 (2001).